U.S. Department of Transportation

Federal Railroad Administration

Investigation of Wheel and Rail Rolling Contact Fatigue Using a Full-Scale Simulator

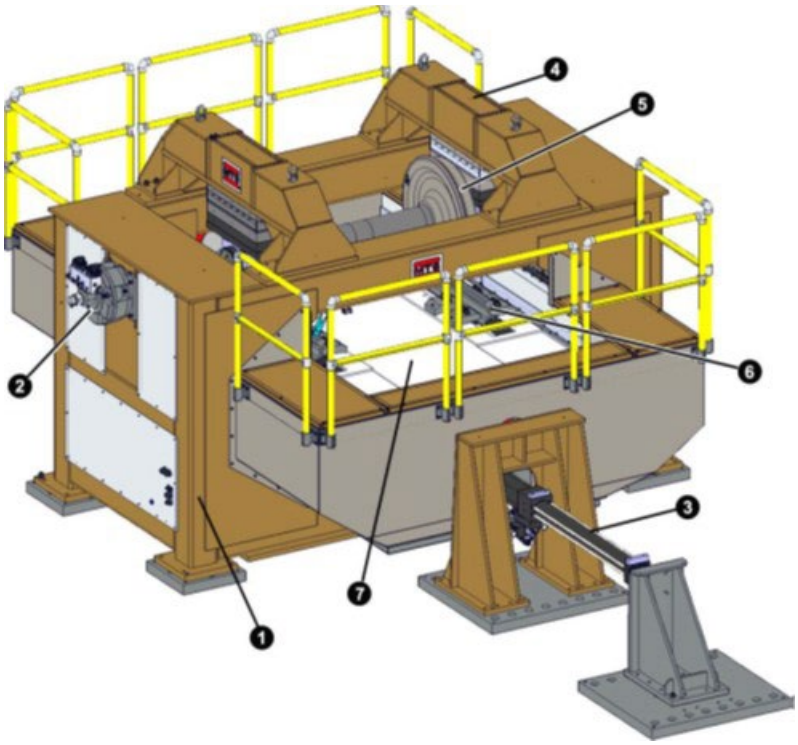

DOT/FRA/ORD-22/13

Final Report
March 2022

REPORT DOCUMENTATION PAGE

Form Approved
OMB No. 0704-0188

1. AGENCY USE ONLY (Leave blank)	2. REPORT DATE	3. REPORT TYPE AND DATES COVERED
	March 2022	Technical Report, 2015–2016

4. TITLE AND SUBTITLE
Investigation of Wheel and Rail Rolling Contact Fatigue Using a Full-Scale Simulator

5. FUNDING NUMBERS
DTFR53-11-D-00008
Task Order 349

6. AUTHOR(S)
Harry Tournay, Xinggao Shu, Alexander Keylin, Sabri Cakdi

7. PERFORMING ORGANIZATION NAME(S) AND ADDRESS(ES)
Transportation Technology Center, Inc.
55500 DOT Road, Pueblo, Colorado, 81001

8. PERFORMING ORGANIZATION REPORT NUMBER

9. SPONSORING/MONITORING AGENCY NAME(S) AND ADDRESS(ES)
U.S. Department of Transportation
Federal Railroad Administration
Office of Research, Development, and Technology
Washington, DC 20590

10. SPONSORING/MONITORING AGENCY REPORT NUMBER
DOT/FRA/ORD-22/13

11. SUPPLEMENTARY NOTES
COR: Ali Tajaddini

12a. DISTRIBUTION/AVAILABILITY STATEMENT
This document is available to the public through the FRA website.

12b. DISTRIBUTION CODE

13. ABSTRACT (Maximum 200 words)
With support from FRA, Transportation Technology Center Inc. (TTCI) developed a full-scale rolling contact fatigue simulator (RCFS) to research the root causes of wheel and rail surface damage. This damage comprises surface pitting, cracking, wear, and material flow and is a function of both the vertical wheel load (and normal contact stresses) and the steering tractions transmitted across the contact patch. The RCFS can simulate nominal axle loads of up to 49.5 tons. The position and orientation of the wheelset to the track (i.e., angle-of-attack and lateral displacement from the track centerline) can be adjusted to control the steering forces on both high and low rails. High steering tractions on the low rail have been found to develop high-impact wheel and rail damage. TTCI's task was to determine the limits to these tractions and, in turn, set performance limits for bogies in heavy haul operation in North America. This report describes how the RCFS operates as well as the supporting analysis and initial tests to develop wheel and rail damage on the low rail as part of this effort.

14. SUBJECT TERMS
Rolling contact fatigue, RCF, rolling contact fatigue simulator, RCFS, high-impact wheel, HIW, wheel and rail defects, wheel and rail forces

15. NUMBER OF PAGES
30

16. PRICE CODE

17. SECURITY CLASSIFICATION OF REPORT	18. SECURITY CLASSIFICATION OF THIS PAGE	19. SECURITY CLASSIFICATION OF ABSTRACT	20. LIMITATION OF ABSTRACT
Unclassified	Unclassified	Unclassified	

NSN 7540-01-280-5500
Standard Form 298 (Rev. 2-89)
Prescribed by ANSI Std. 239-18
298-102

METRIC/ENGLISH CONVERSION FACTORS

ENGLISH TO METRIC	METRIC TO ENGLISH
LENGTH (APPROXIMATE)	**LENGTH (APPROXIMATE)**
1 inch (in) = 2.5 centimeters (cm)	1 millimeter (mm) = 0.04 inch (in)
1 foot (ft) = 30 centimeters (cm)	1 centimeter (cm) = 0.4 inch (in)
1 yard (yd) = 0.9 meter (m)	1 meter (m) = 3.3 feet (ft)
1 mile (mi) = 1.6 kilometers (km)	1 meter (m) = 1.1 yards (yd)
	1 kilometer (km) = 0.6 mile (mi)
AREA (APPROXIMATE)	**AREA (APPROXIMATE)**
1 square inch (sq in, in^2) = 6.5 square centimeters (cm^2)	1 square centimeter (cm^2) = 0.16 square inch (sq in, in^2)
1 square foot (sq ft, ft^2) = 0.09 square meter (m^2)	1 square meter (m^2) = 1.2 square yards (sq yd, yd^2)
1 square yard (sq yd, yd^2) = 0.8 square meter (m^2)	1 square kilometer (km^2) = 0.4 square mile (sq mi, mi^2)
1 square mile (sq mi, mi^2) = 2.6 square kilometers (km^2)	10,000 square meters (m^2) = 1 hectare (ha) = 2.5 acres
1 acre = 0.4 hectare (he) = 4,000 square meters (m^2)	
MASS - WEIGHT (APPROXIMATE)	**MASS - WEIGHT (APPROXIMATE)**
1 ounce (oz) = 28 grams (gm)	1 gram (gm) = 0.036 ounce (oz)
1 pound (lb) = 0.45 kilogram (kg)	1 kilogram (kg) = 2.2 pounds (lb)
1 short ton = 2,000 pounds (lb) = 0.9 tonne (t)	1 tonne (t) = 1,000 kilograms (kg)
	= 1.1 short tons
VOLUME (APPROXIMATE)	**VOLUME (APPROXIMATE)**
1 teaspoon (tsp) = 5 milliliters (ml)	1 milliliter (ml) = 0.03 fluid ounce (fl oz)
1 tablespoon (tbsp) = 15 milliliters (ml)	1 liter (l) = 2.1 pints (pt)
1 fluid ounce (fl oz) = 30 milliliters (ml)	1 liter (l) = 1.06 quarts (qt)
1 cup (c) = 0.24 liter (l)	1 liter (l) = 0.26 gallon (gal)
1 pint (pt) = 0.47 liter (l)	
1 quart (qt) = 0.96 liter (l)	
1 gallon (gal) = 3.8 liters (l)	
1 cubic foot (cu ft, ft^3) = 0.03 cubic meter (m^3)	1 cubic meter (m^3) = 36 cubic feet (cu ft, ft^3)
1 cubic yard (cu yd, yd^3) = 0.76 cubic meter (m^3)	1 cubic meter (m^3) = 1.3 cubic yards (cu yd, yd^3)
TEMPERATURE (EXACT)	**TEMPERATURE (EXACT)**
[(x-32)(5/9)] °F = y °C	[(9/5) y + 32] °C = x °F

QUICK INCH - CENTIMETER LENGTH CONVERSION

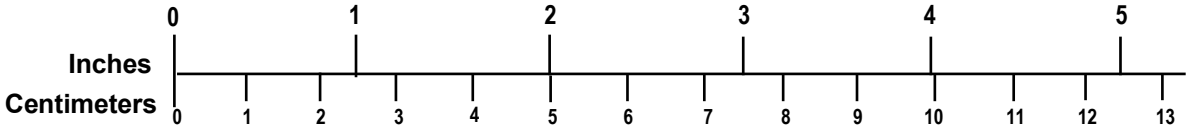

QUICK FAHRENHEIT - CELSIUS TEMPERATURE CONVERSIO

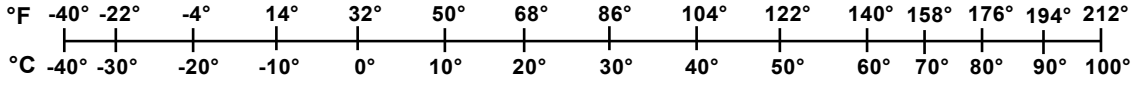

For more exact and or other conversion factors, see NIST Miscellaneous Publication 286, Units of Weights and Measures. Price $2.50 SD Catalog No. C13 10286

Updated 6/17/98

Acknowledgements

The Federal Railroad Administration (FRA) Office of Research, Development, and Technology and the Association of American Railroads' Strategic Research Initiatives program jointly funded the research described in this report .

Thanks go to Ali Tajaddini of FRA and Brian Marquis of the Volpe Center for their technical discussions.

EVRAZ North America provided the test rails.

Contents

Illustrations

Executive Summary

Transportation Technology Center Inc. (TTCI) built a rolling contact fatigue simulator to study wheel and rail contact, including damage initiation and wear. The Federal Railroad Administration (FRA) supported this work. In 2015–2016, researchers conducted exploratory tests under nominal (35,750-lb.) wheel loads and traction ratios (T/N) of 0.1, 0.2, 0.3, and 0.4 and using different wheel and rail materials. Under dry contact, the researchers found the following:

- Surface damage started within about 20,000 cycles, after which it remained substantially constant as the surfaces wear, suggesting an optimal test duration ≈ 20,000 cycles.
- Presumed critical damage, in the form of surface pitting, occurred in the range T/N ≈ 0.15 through 0.3, above which an abrasive wear regime wore away the pitting as it formed.
- For Class C wheel material, a point of inflection occurred for wear between pitting and abrasive wear between T/N ≈ 0.2 and 0.3.

The research team tested for modeling contact stresses using unworn 36-inch AAR1B wheel and AREMA 136RE rail under 36-ton axle load and unlubricated conditions. Their findings include:

- A typical low rail tangential force environment for a lead axle of a non-steering truck on an unlubricated track was damaging. Permanent surface deformation developed on the surfaces of both the wheel and the rail. This occurred on Class C wheel and intermediate strength rail at 0.1 T/N (occurred on 2-degree and sharper curves). It also occurred on the surface of high-strength rail at 0.2 T/N (occurred on 3-degree and sharper curves).
- When tangential forces were zero, the maximum subsurface equivalent stress of about 106 ksi occurred approximately 3/16 inch below the surface. Subsurface von Mises stresses were slightly above Class C and below Class D wheel yield strengths. Intermediate-strength rail and high-strength rail yield strengths were higher than the subsurface von Mises stresses.

During the project, researchers proposed to determine the surface roughness (depth of pitting), rate of wear, and point of inflection of wear for Class C and Class D wheels more accurately. The experiments covered the following items for low rail contact condition:

- Class C (reported in this report) and D wheels
- Balance and 3-inch underbalance conditions
- Finer T/N intervals with improved (more accurate) surface condition and wear measurement up to ≈ 20,000 cycles for T/N = 0.125; 0.150; 0.175; 0.200; 0.225; 0.250; 0.275. These refined intervals were within the control capabilities of the RCFS.
- Finer measurement and quantification of the surface damage
- Simulation of the seasonal effects of snow, using an artificial third body layer

Researchers determined the T/N limits for surface damage between the two wear regimes of burnishing (presumed T/N < 0.15) and abrasive wear (presumed T/N > 0.3) from those proposed

tests. Results from these added tests helped determine the optimal T/N limits for the freight car truck to avoid or substantially reduce the incidence of HIW and reduce low rail RCF damage in curves.

1. Introduction

Transportation Technology Center Inc. (TTCI) developed a full-scale rolling contact fatigue simulator (RCFS) to research the root causes of wheel and rail surface damage. The Federal Railroad Administration (FRA) and the Association of American Railroads'(AAR) Strategic Research Initiative (SRI) program jointly funded the project.

This research is an ongoing multiyear project. This report summarizes the tests and modeling work completed in 2016 and presents preliminary findings.

1.1 Background

Previous studies [1,2] have associated high-impact wheels (HIW) and rail spalling to rolling contact fatigue (RCF) at the interface between the wheel tread and the rail surface (see Figure 1). Wheel and rail RCF result in reduced wheel and rail life and increased maintenance costs. RCF has emerged as a governing reason for rail replacement and maintenance and for rail failure and safety concerns. HIWs are the primary driver of wheelset removals, which are consistently more than half of the rolling stock maintenance cost for Class I railroads.

Figure 1. Wheel and rail RCF

TTCI's task was to explore the root causes of wheel and rail damage and to suggest design, maintenance, and operating strategies to mitigate this damage. This damage is comprised of surface pitting, cracking, wear, and material flow, either individually or in combination. It is a function of both the vertical wheel load (and normal contact stresses) and the steering tractions transmitted across the contact patch. In support of this task, TTCI has commissioned and

acquired a rolling contact fatigue simulator (RCFS) in support of analytical approaches in contact mechanics.

So far, tests have been conducted under nominal 36-ton axle loads and variable steering tractions using wheels with Class C and Class D materials on intermediate-strength rails. The focus of this work has been to gain experience with the experimental approach and, later, to determine the limits to steering tractions on low rail contact. High steering tractions from low rail contact have been determined to be the driver of the development of HIW and associated low rail damage in North America [3].

1.2 Objectives

The objective of this RCF research program is to develop effective wheel/rail interface management strategies to mitigate safety risks and financial burdens of RCF.

1.3 Overall Approach

Experimental and analytical approaches were used to investigate the root cause of RCF. The experimental approaches included RCF tests using the RCFS and revenue service on-track tests using load measuring, strain gaged wheelsets (also known as instrumented wheelsets, or IWS).

The analytical approach included modelling wheel and rail contact using the CONTACT [4] program and finite element analysis (FEA) software. Modeling of rolling contact stresses under various vertical loading, wheel and rail profiles, friction coefficients, and tangential forces is essential to predict wheel and rail contact stresses on the surface and subsurface. The surface damage was predicted by using the shakedown criterion. Once the RCFS tests confirmed the modelling results; the team then used the validated model to design test regimes for RCFS tests and on-track tests in revenue service.

1.4 Scope

The scope of the work included:

- RCFS installation and documentation, including its test functions, capabilities, and operation procedures
- RCF tests to investigate effects of the following factors on wheel and rail RCF:
  - Wheel/rail traction ratios (T/N)
  - Wheel loads
  - Rail material (intermediate- and high-yield-strength rails)
  - Wheel material (Class C and D wheels)
  - Third body layer (lubricant) between wheel and rail
- RCFS tests to measure wheel and rail contact forces with different wheel and rail combinations, at different angles of attack (AOA) and axle lateral shift positions

1.5 Organization of the Report

This report contains five sections. Section 1 covers the background of this study while Section 2 discusses the test functions and capabilities of RCFS. Section 3 outlines how the researchers

determined the limits to the lead axle low rail (LALR) steering tractions. Section 4 presents the wheel/rail (W/R) contact stress modeling work and Section 5 discusses findings from this study and recommendations.

2. RCFS Test Functions and Capabilities

The RCFS (Figure 2) is a hydraulic test machine containing a full-scale wheelset rolling on the two rails fixed to a longitudinally reciprocating table that simulates a standard gage track.

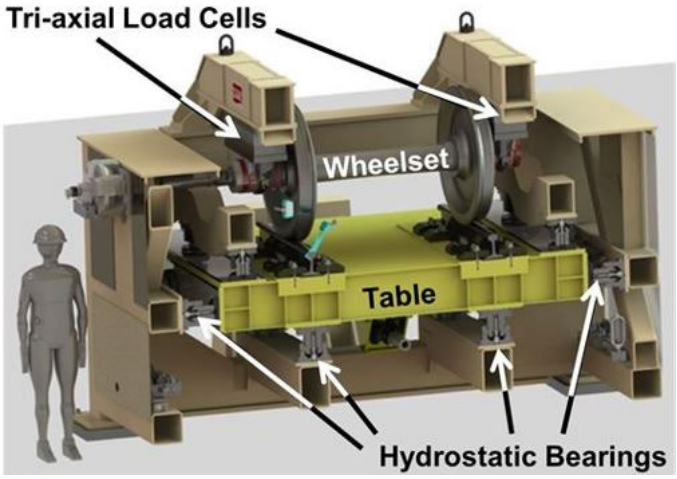

Figure 2. Schematic of RCFS

The wheelset is fixed rigidly to the rig frame through tri-axial load cells. Rotation through the journal bearings was the only degree-of-freedom the wheelset had relative to the rig frame.

The rails are rigidly fixed to a reciprocating table. This table is loaded and guided by hydrostatic bearing/actuator combinations. The vertical actuators apply a vertical load from the table (and rails/track) to the wheelset. The lateral actuators control the lateral and yaw orientation (AOA) between the table, and, thus, the rails/track, and the wheelset.

The table (track) is reciprocated under the wheelset. This motion is activated by a long stroke longitudinal actuator (Figure 3).

Figure 3. Reciprocating table activated by a longitudinal actuator

The table can be cyclically raised and lowered to engage and load the wheelset to simulate either unidirectional or bidirectional running.

The table can apply a net nominal axle load up to 49.5 tons and can apply differential wheel loads to simulate overbalance and underbalance conditions.

In summary, the RCFS provides the following test capabilities:

- Full-scale wheelset (28-inch to 41-inch diameter) rolling on a full-scale pair of rails (115 lbs/yard to 143 lbs/yard), a standard gage distance apart
- 72,000 lbs (36-ton axle load) vertical, 84,000 lbs lateral, 20,000 ft-lb yaw (AOA) torque and 44 milliradian (mRad) yaw angle capacity
- A 4-foot stroke with 6 degrees-of-freedom rail carriage table motion and 1 degree-of-freedom (rotation) wheelset motion at approximately 3.5 mph with high accuracy displacement, angle, force and moment control, and measurements (<1% at full capacity)
- Laser-based profile measurement systems and cameras for each wheel and rail to monitor the wear and surface damage progression.
- Unidirectional and bidirectional (combination of empty and loaded cars) curving simulation at underbalance, overbalance, or balance speed with flanging or non-flanging conditions
- Validation of multibody simulation software packages and RCF models. Calculations that can be confirmed include prediction of wheel and rail forces, contact patch geometry and location, damage mode, rate, and life cycles for various test conditions

The following features are planned to be available soon by modifying the control code and integrating peripheral systems to RCFS:

- Up to four different AOAs and lateral positioning of the test wheelset in one command loop to simulate entire four-axle car curving
- Testing the effects of any available third body layer substance on traction, friction, and damage (e.g., RCF, wear, corrugation, etc.) such as, friction control products, water, ice, and leaves
- Test functions of the effects of elevated temperatures on wheel tread damage due to thermal loads during braking

Lateral creep forces are developed by controlling the AOA of the rails and table with respect to the wheelset (Figure 4).

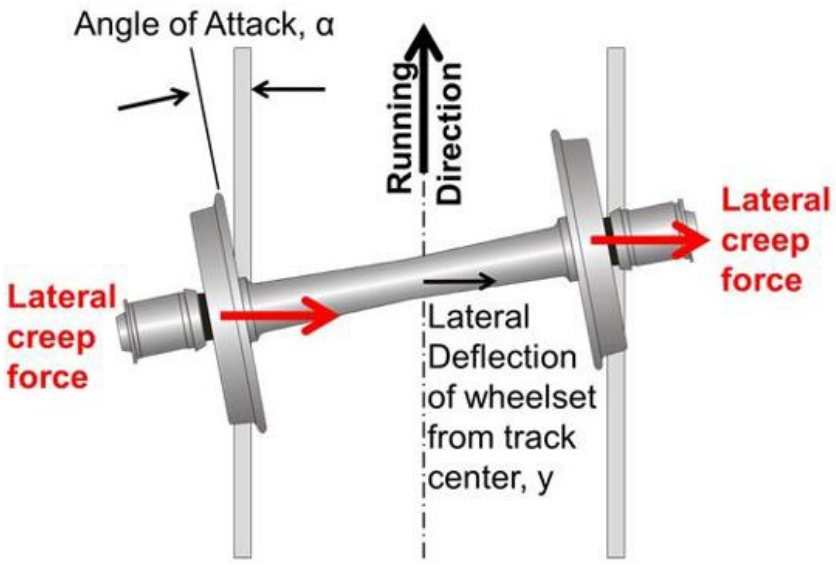

Figure 4. Measured lateral creep forces on the wheelset

Lateral creep force is directly proportional to the AOA. Figure 5 shows test results of the typical net lateral creep force on the wheelset under a 36-ton axle load versus AOA for a wheelset centrally placed on the track (y = 0). Under these conditions, a conical wheel profile exerts no net lateral gravitational force due to the angles of the plane of the contact patch to the axis of the axle. The hydrostatic bearings and associated actuators generate the reaction forces to these lateral creep forces.

Flange forces can be a product of the lateral creep forces. If the hydrostatic bearings and associated actuators do not react the lateral creep forces, the table will displace laterally into flange contact, generating flange forces.

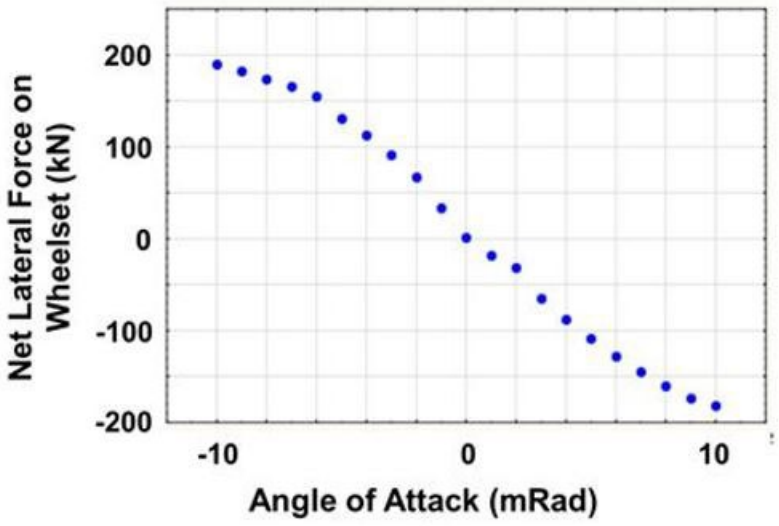

Figure 5. Net lateral force on wheelset versus AOA

Longitudinal creep force is proportional to the radius differential generated between the wheels of the wheelset. This force is proportional, in turn, to the lateral displacement of the wheelset (Figure 6).

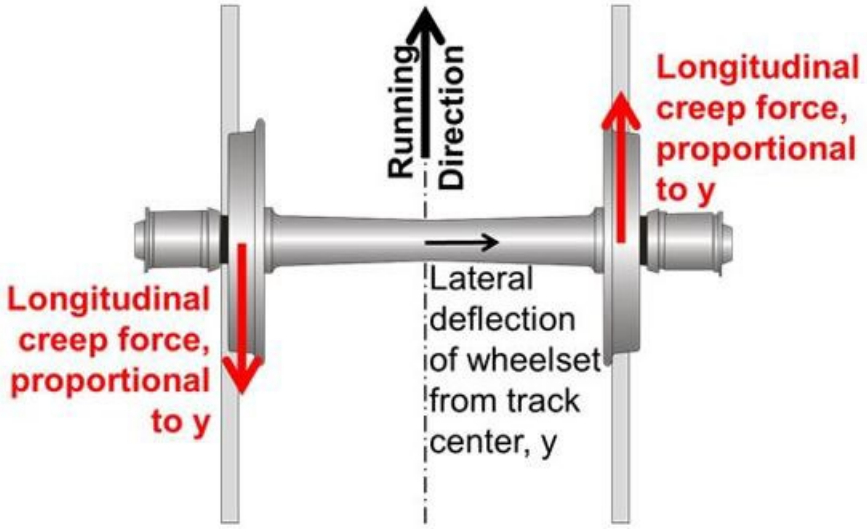

Figure 6. Longitudinal creep forces

Figure 7 shows typical test results of the net longitudinal force at each contact patch as a function of wheelset lateral displacement from the track centerline. The left and right wheel longitudinal forces cross at a position with about 3 mm lateral displacement from track center, where rolling radii of two wheels are equal. The net moment generated by the longitudinal creep forces is reacted at the hydrostatic bearings and associated actuators.

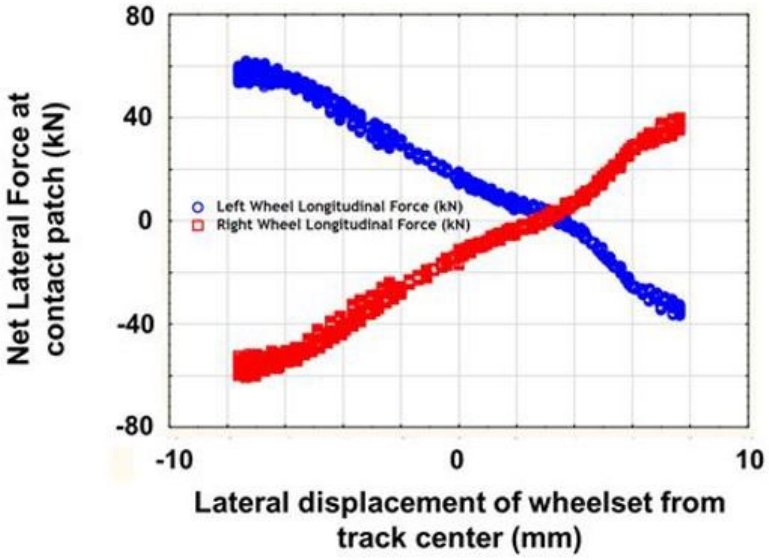

Figure 7. Measured longitudinal creep force at each contact patch

The T/N under each wheel can be calculated from the measured dynamic longitudinal, lateral, and vertical wheel/rail forces. In addition to the force measurements, the following parameters were measured and recorded periodically after certain amounts of reciprocal cycles:

- Roughness on the wheel and rail surfaces measured by a portable roughness tester.
- Hardness on the wheel and rail surfaces measured by a portable hardness tester.
- Wheel and rail profiles measured by a portable profilometer and laser system.
- Wheel and rail surface pictures with dye penetration

3. Determination of Limits to the LALR Steering Tractions

The research team concluded that controlling the position and orientation of the reciprocating table to the wheelset can control the creep forces. Extended testing beyond 200,000 cycles has shown this to be generally true. However, the table lateral position and yaw angle must be adjusted during extended testing to keep the creep force constant, especially when significant wear occurs.

The formation of HIW has been associated with lead axle, low rail steering tractions developed by bogies in curves [5-9]. A so-called improved freight car truck (bogie), or integrated freight car truck (IFCT), has been proposed to reduce these tractions [9]. Researchers developed a test procedure to evaluate bogie steering performance using the LALR T/N [1]. The missing element in this development is the determination of the limits to the LALR T/N. The RCFS is being used to determine these limits for 36-ton axle loads and prevailing and future wheel steels in North American revenue service.

3.1 Test Approach

TTCI quantified the levels of LALR T/N developed in curves and the relationship between the longitudinal and lateral creepages under these conditions [1,9]. Figure 8 shows, diagrammatically, the LALR T/N.

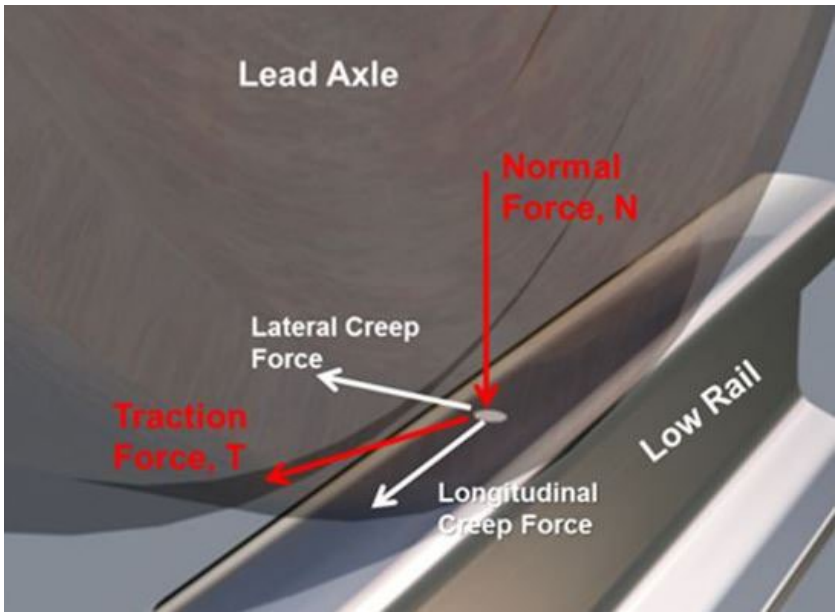

Figure 8. LALR T/N

This LALR T/N metric is the vector sum of the longitudinal and lateral creep forces developed by the lead axle in the plane of the low rail contact patch divided by the normal load acting on the contact patch.

The RCFS was configured to produce LALR T/N, under a 36-ton axle load for balance conditions, for T/N values of 0.1, 0.2, 0.3, and 0.4. Class C wheels and intermediate-strength rails were used in the test reported in this paper. TTCI will report on other wheel and rail

combinations used in the future. Low rail contact is made between the conical portion of a typical North American wheel profile and the rail head with an approximate 250 mm crown profile radius. Figure 9 shows the test regime for Class C material as represented on a shakedown map for partial slip (dry contact).

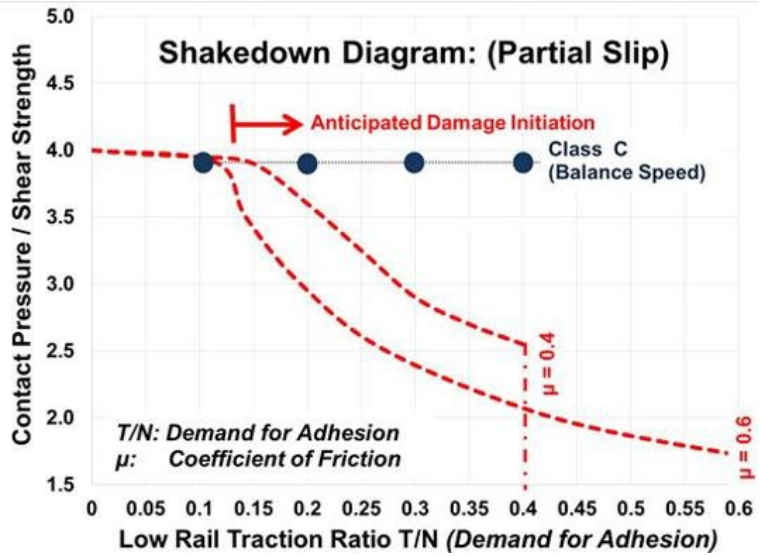

Figure 9. Shakedown map, Class C wheel, 36-ton axle loads

Figure 9 shows the shakedown map for coefficients of friction of 0.4 and 0.6. Class C and intermediate strength rail tests suggested the prevailing coefficients of friction under the laboratory conditions of the RCFS were in this range. Total slip was seen under a demand for adhesion greater than approximately 0.55.

The shakedown map suggested that surface damage should initiate under LALR T/N greater than approximately 0.13.

3.2 Test Observations and Results

Figure 10 shows an overview of the observations from tests on a Class C wheel at LALR T/N of 0.1, 0.2, 0.3, and 0.4 and superimposed on the shakedown map.

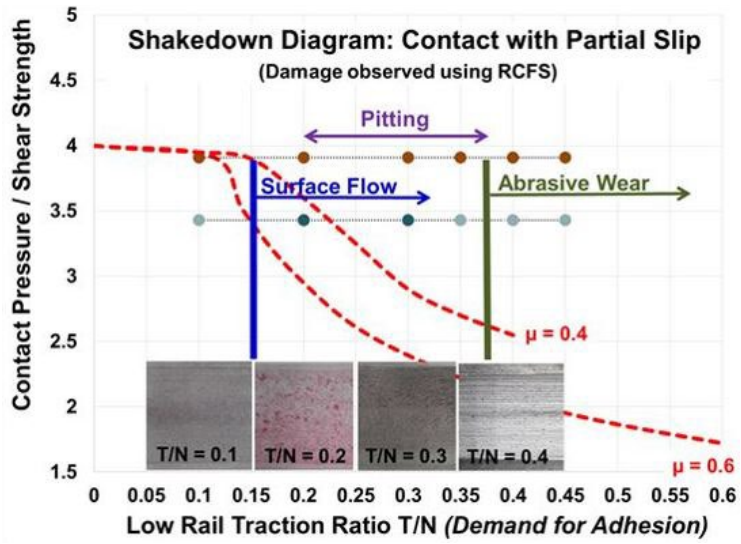

Figure 10. Observations from tests of Class C wheel material

Figure 11 shows detail of typical surface damage at the LALR T/N values tested.

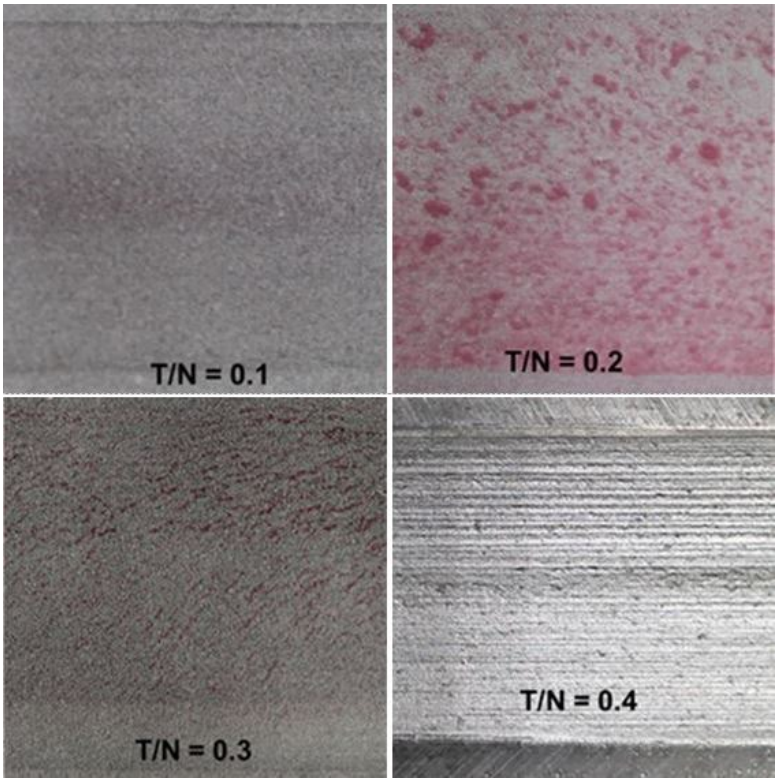

Figure 11. Detailed images of typical surface damage on a Class C wheel under 36-ton axle loads at balance speed and with typical profiles in low rail contact

Observations made during the tests:

- The width of the contact band was similar to that predicted by the Hertz theory.
- Damage, in the form of pitting:

  - Initiates between a T/N (demand for adhesion) of 0.1 and 0.2
  - Initiates rapidly after, generally, between 10,000 and 20,000 cycles
- Reached a steady state condition after this rapid initiation, "moving" into the wheel surface with the wear of the wheel up to the maximum of 250,000 cycles tested.
- Light surface spalling observed on the low rail and the wheel tread initiated between a T/N of 0.2 and 0.3. The striations from this light spalling were generally at right angles to the applied tractions. The light spalling occurred at T/N ≈ 0.3 *may* have been the initiator of surface damage on the wheel leading to HIW. Further tests are needed to verify the T/N ratio.
- Abrasive wear initiated between a T/N of 0.3 and 0.4. The surface of the wheel became "grooved," presumably as debris initiating from the pitting/light spalling/striations was rolled through the region of slip.
- As pointed out above, the damage initiated rapidly and reached a steady state; wear then started to alter the contact geometry. Thus, ideal test durations under dry contact are likely to be about 20,000 to 30,000 cycles. As contact repeatedly occurs on the same contact band, this can translate into more effective net cycles on a wheel tread than indicated or implied by 20,000 to 30,000 cycles.

Figure 12 shows the wheel wear depth plotted against effective number of cycles.

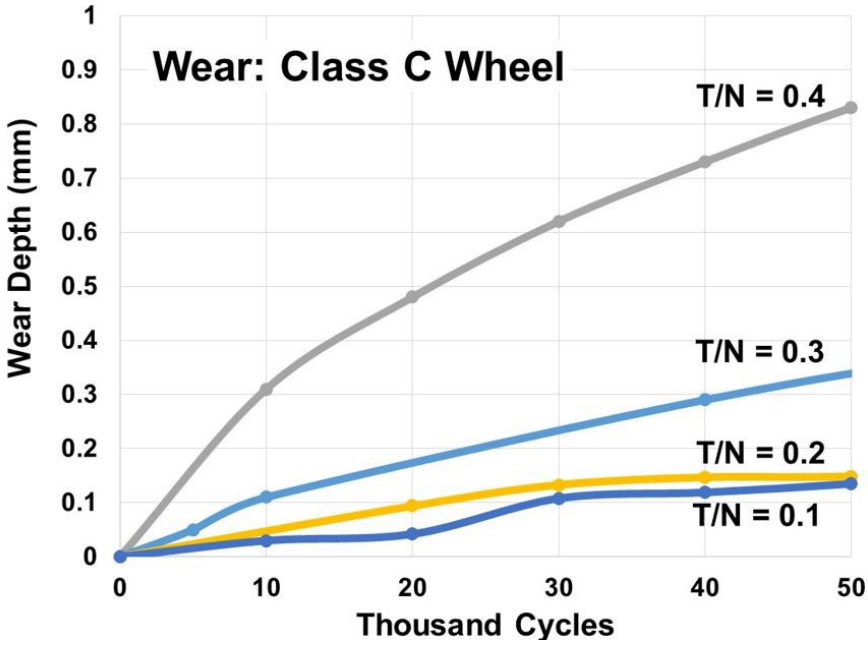

Figure 12. Wear depth versus load cycles

The initial wear rate was high for higher demands for adhesion. This rate "flattened" as the wheel wore into more conformal contact with the rail.

Figure 13 shows the initial measured wear rates shown in Figure 12 and plotted on the shakedown diagram.

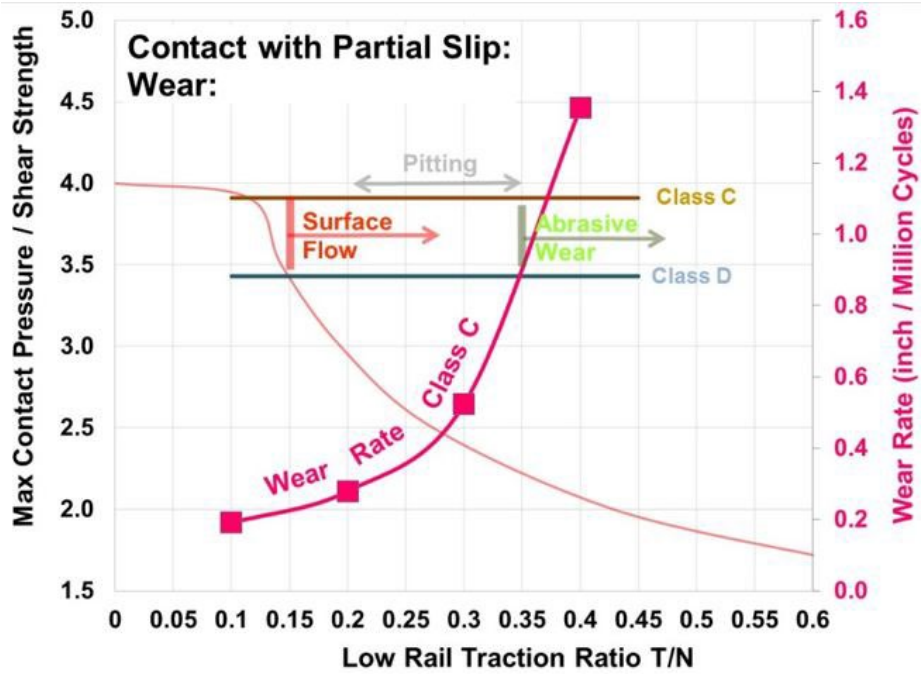

Figure 13. Initial wear rates developed from the Figure 12 graphs and plotted on the shakedown map

Figure 13 suggests the point of inflection between T/N = 0.2 and T/N = 0.3, where the wear rate on the wheel was significantly increased in line with the observations shown in Figure 11.

3.3 Discussion of Test Results

Initial tests suggested that light spalling was generated on a Class C wheel tread at T/N ratios ≈ 0.3. This T/N regime *may* have been the initiator of HIW. Further tests are needed to verify the T/N ratio.

For 0.1 > T/N < 0.3, a regime of pitting occurred that may or may not play a role in HIW formation.

For T/N ≥ 0.3, an abrasive wear regime initiates that appears to wear away the pitted / light spalling wheel material noted at lower T/N ratios. Researchers did not consider wear rates for T/N ≥ 0.3 candidates for HIW damage initiation, as the surface on which damage was initiated was worn away.

Surface damage (pitting/light spalling) reached steady-state conditions and did not develop into the surface crack growth observed on wheel treads in revenue service (Figure 14).

Different, non-constant T/N load regimes were simulated to further develop pitting/light spalling into initiated cracks. These generally focused on initiating pitting/light spalling under T/N ≈ 0.3and then changing to lower T/N to develop and propagate surface cracks. The sequencing of the test tried to simulate the wheel spalling initiated by low rail contact on a curves, then crack propagation on the wheel when it runs on tangent tracks.

These attempts proved unsuccessful; the pitting/light spalling was “flattened” into the surface of the wheel and eventually worn away under the relatively low wear T/N regimes.

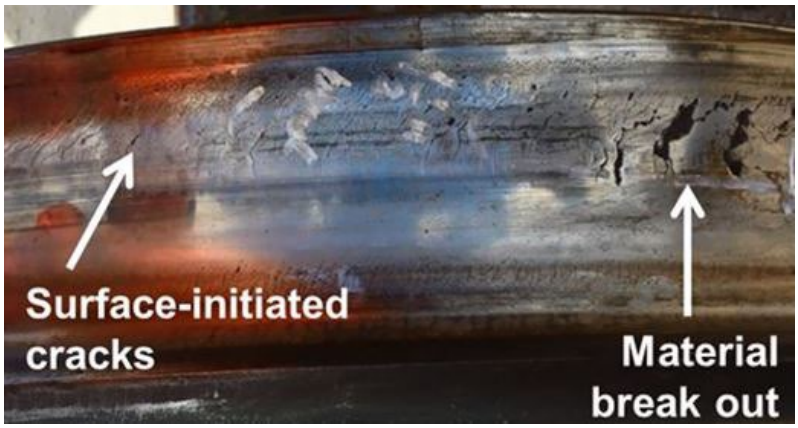

Figure 14. Surface damage associated with HIW

More HIWs are detected during winter in North America, especially in snowy conditions (Figure 15). Testing in dry contact (under high friction coefficients) conditions will not explain the seasonality of HIW formation.

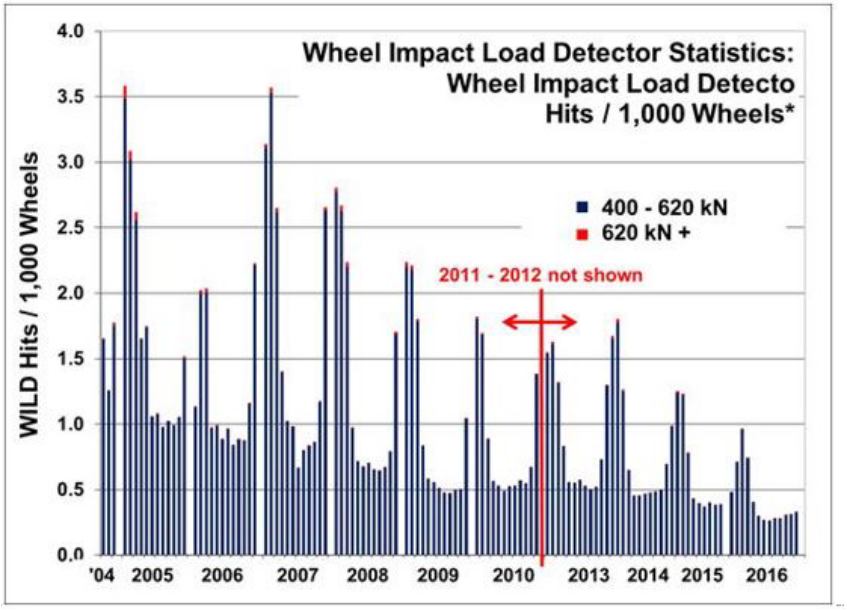

Figure 15. Seasonality of HIW in North America

It was evident that another mechanism was likely needed to further develop surface pitting/light spalling into crack initiation and growth. This mechanism, associated with the formation of hydraulic pressure in surface cracks (or surface pits/light spalling), has been reported in the literature on RCF. It has been used in procedures associated with developing damage in twin-disk test procedures [10].

The possible service failure mechanism may thus be pitting/light spalling under dry contact and followed by a third body layer (such as snow) pressed into the damaged surface. The resulting hydraulic pressure would then produce tensile stresses in a dominantly compressive surface contact stress regime to initiate cracking (Figure 16). Test procedures are being developed and

planning/design is underway to verify the hydraulic effect of water (from rain/snow) on HIW formation.

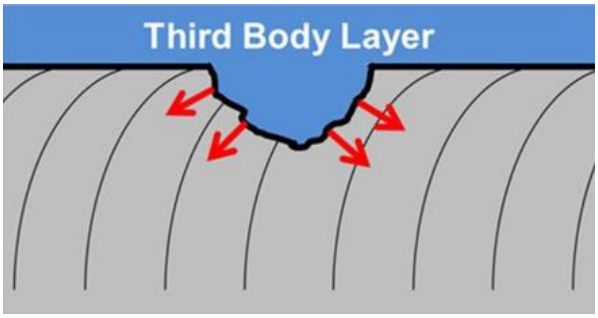

Figure 16. Pressure in the third body layer creating tensile stresses in the pits and light spalling generated under dry contact

Tests also indicated the need for:

- Finer T/N test intervals to more precisely determine the region of observed pitting/light spalling and the break point for abrasive wear. Figure 17 shows the planned test tractions on the shakedown map. This refined test interval is within the control capabilities of the RCFS.
- More accurate measurement/quantification of surface roughness condition. Microscopic laser surface roughness and pitting depth measurement approaches are being investigated.

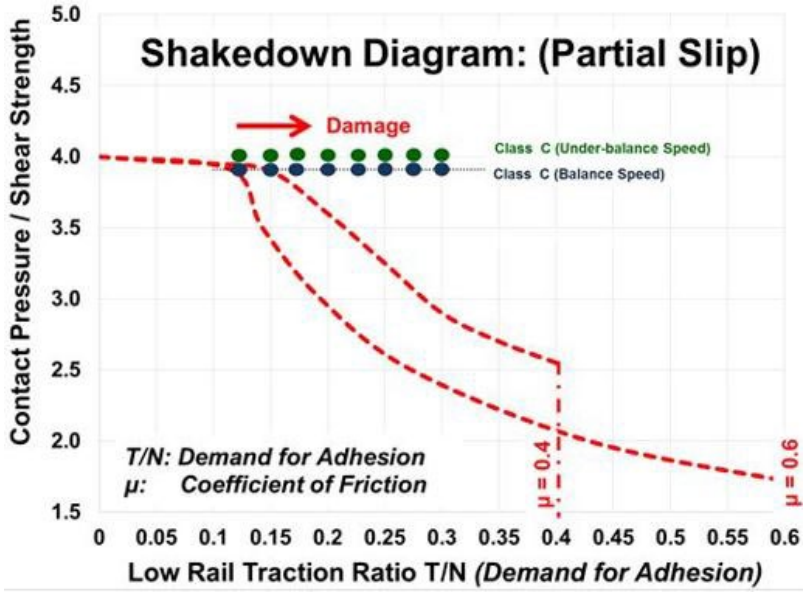

Figure 17. Propose test regime for finer determination of damage limits

4. Contact Stress Modeling

High steering tractions in low rail contact have been found to develop HIW and low rail damage. To improve understanding of material flow, wear, crack initiation, and growth, TTCI conducted a study of wheel and rail contact stresses under a leading axle of a nonsteering freight truck with 36-ton axle loads. Force inputs measured with IWS in a field test [1] served as inputs for linear elastic models in CONTACT [4] and the FEA software, ANSYS.

Curving tests at the Transportation Technology Center's (TTC) Wheel/Rail Mechanism (WRM) unlubricated loop provided the force input environment. Tests used a 36-ton axle load and balance speed [1]. Wheel and rail forces were measured via IWS. Figure 18 shows the LALR wheel T/N as a function of degree-of-curvature under nonsteering truck and 36-ton axle loads. Boxes show 25th and 75th percentiles, while whiskers show 1 to 99 percentiles. Median values are connected via lines from tangent to 10-degree curve.

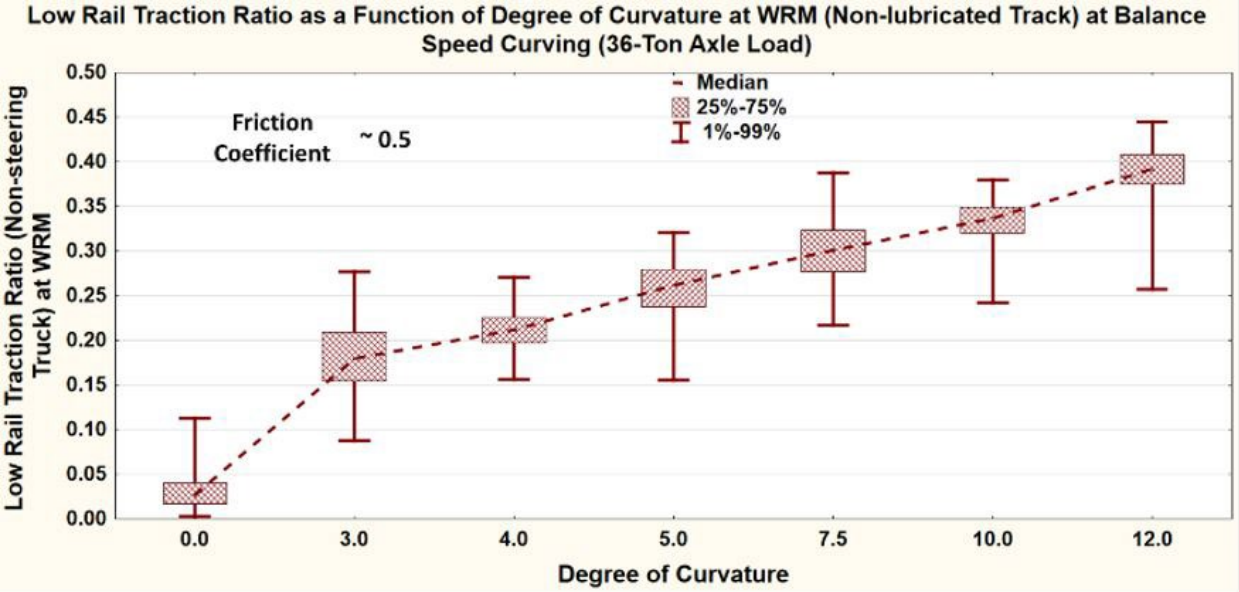

Figure 18. Low rail T/N of nonsteering truck (286,000-lb hopper, unlubricated track, balance speed curving)

Figure 19 shows lateral and longitudinal forces in a similar way. Median lateral forces increased between 3- and 10-degree curves with a near-linear relationship, while longitudinal forces stayed similar between 3- and 10-degree curves. The median lateral and longitudinal forces in the bodies of 3-, 4-, 5-, 7½-,10-, and 12-degree curves were used as inputs for the contact stress model. The RCFS test program was also established with the same force environment. The IWS test results were compared to preliminary test results from the RCFS.

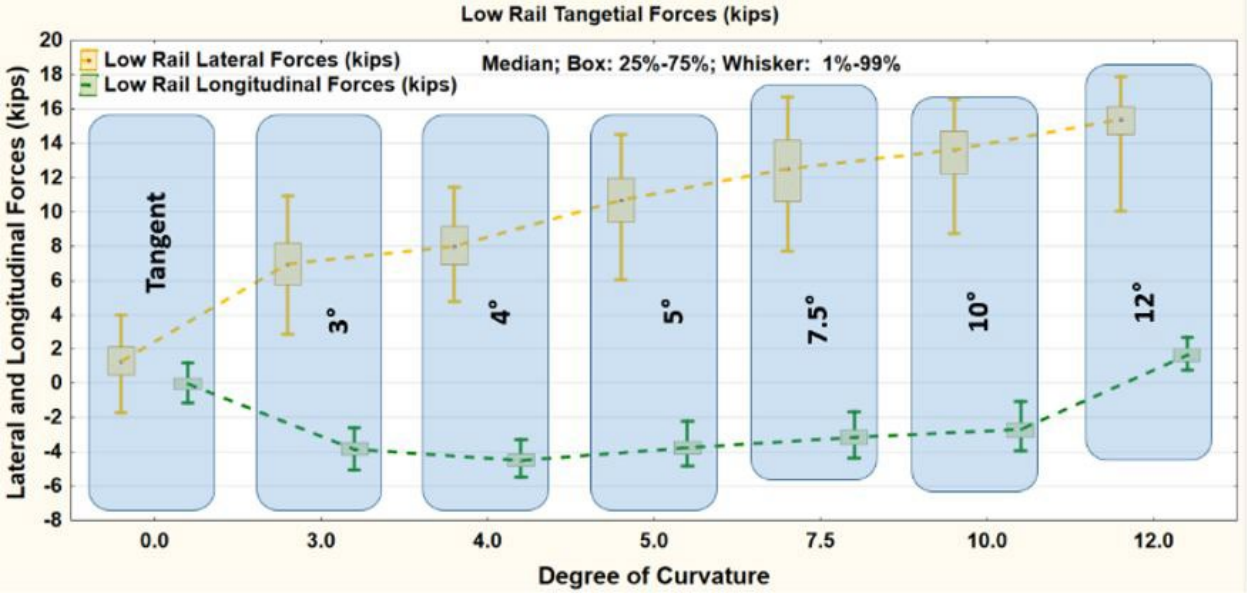

Figure 19. Lateral and longitudinal force of nonsteering truck (286,000-lb hopper, unlubricated track, balance speed curving)

Crack initiation at the wheel and rail surfaces were attributed to the accumulation of plastic deformation (ratchetting) [11]. Thus, quantifying contact stresses under varying load environments that resulted in plastic deformation was critical. In this study, von Mises' theory was used to predict plastic deformation. Operating within an elastic contact stress regime would not eliminate RCF, since fatigue strength was less than yield strength, but it was expected to prolong wheel and rail life. Implementation of complete fatigue life will be investigated in the future.

Low rail contact models showed that the stress distribution difference between CONTACT and FEA software ANSYS was negligible (Figure 20, Figure 21). Since CONTACT is significantly faster than ANSYS, maximum surface and subsurface von Mises stresses were calculated based on median contact forces. Figure 20 shows the von Mises stresses along the vertical plane where maximum surface stresses were generated. Figure 21 shows surface von Mises stresses at the contact patch plane.

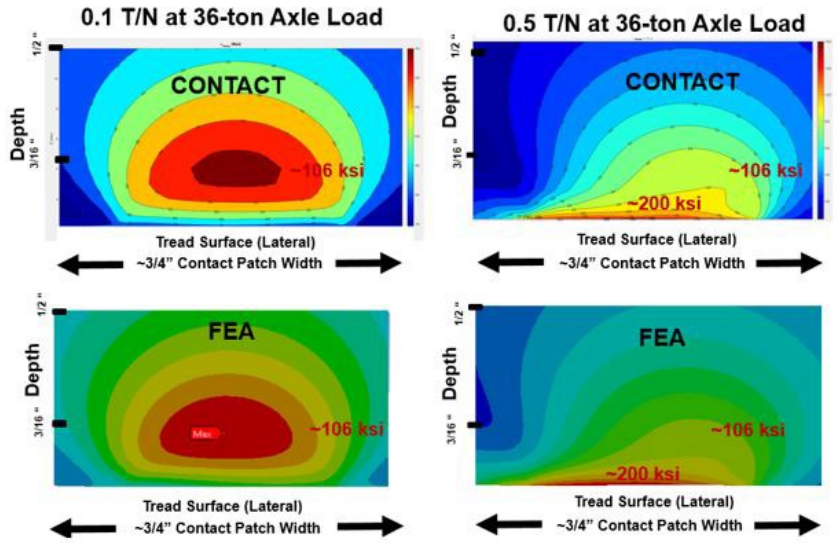

Figure 20. von Mises stress distribution along the vertical plane at the center of contact patch at very low and very high tractions

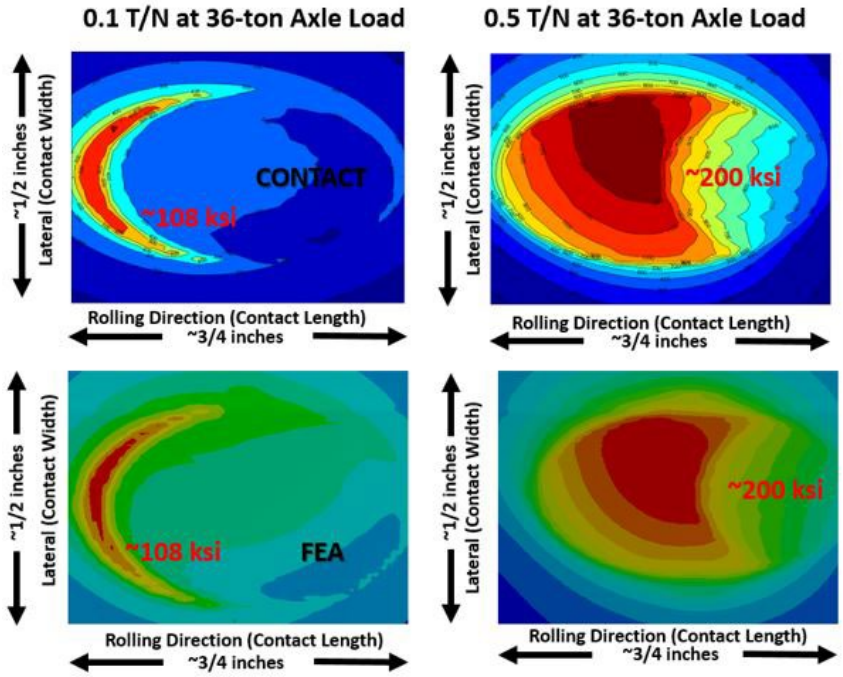

Figure 21. von Mises stress distribution along the contact surface at very low and very high T/N

Figure 22 shows the modeling results of maximum von Mises stresses on the surface and at 3/16 inch below the surface, as a function of T/N under a 36-ton axle load. Maximum surface von Mises stress increased from 38 ksi to 186 ksi with increasing traction forces, and von Mises stresses at 3/16 inch below surface increased slightly from 106 ksi to 114 ksi.

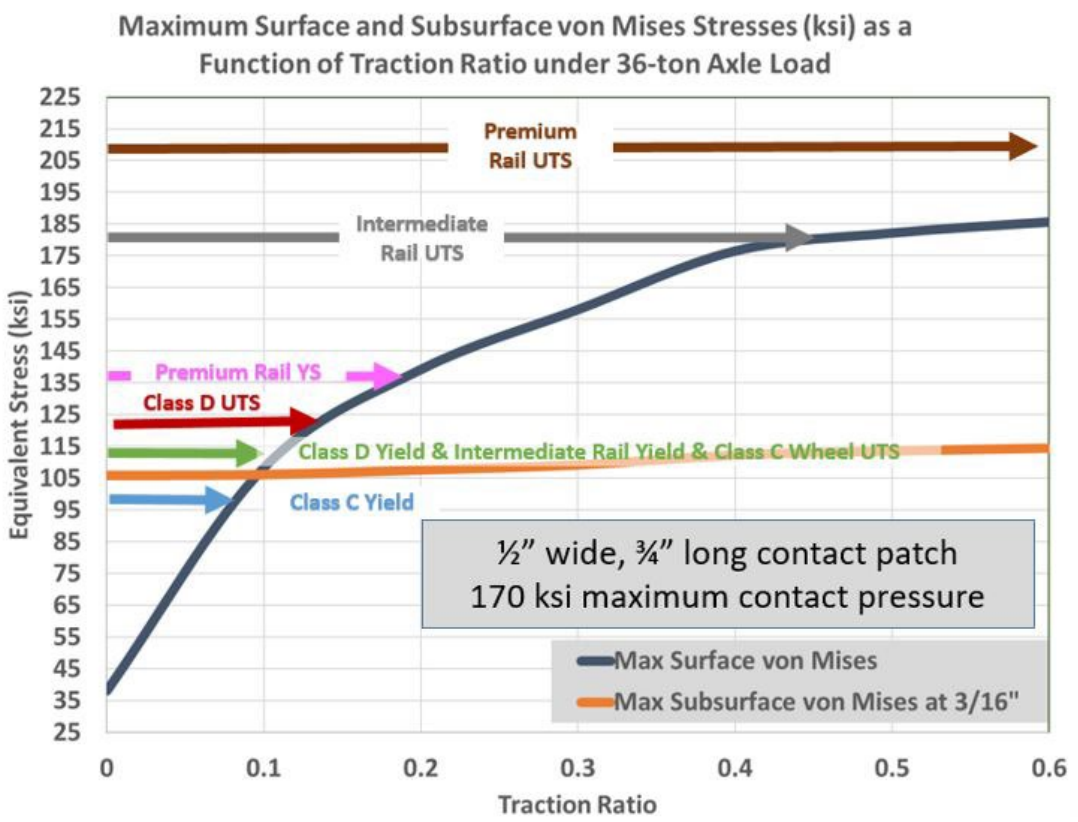

Figure 22. Maximum surface and subsurface von Mises stresses (36-ton axle load, unworn wheel tread and top-of-rail [136RE] profiles)

The modeling results were consistent with the results of RCFS test program. However, the maximum contact pressure, pressure distribution, and resultant surface traction distribution can change with worn wheel and rail profiles and contact location; these cases will be investigated in the future. The following conclusions can be drawn from the modeling results:

- A typical low rail tangential force environment for a lead axle of a nonsteering truck on an unlubricated track was sufficient to result in permanent surface deformation on surfaces of Class C wheel, Class D wheel, intermediate-strength rail at 0.1 T/N (occurred on 2-degree and sharper curves), and high-strength rail at 0.2 T/N (occurred on 3-degree and sharper curves).
- In the absence of tangential forces, maximum subsurface equivalent stress location was approximately 3/16 inch below the surface and its magnitude was about 106 ksi. Subsurface von Mises stresses were slightly above Class C and below Class D wheel yield strengths. Intermediate-strength rail and high strength rail yield strengths were higher than generated subsurface von Mises stresses (Figure 20 and Figure 21).

After validating these results with the RCFS, TTCI aims to provide test results and recommendations to FRA and the industry on T/N ratio limits for bogies in heavy haul operation in North America.

5. Conclusion

TTCI, with support from FRA, constructed an RCFS to study wheel/rail contact, including damage initiation and wear. Exploratory tests under nominal (35,750 lb) wheel loads and T/N of 0.1, 0.2, 0.3, and 0.4, and using different wheel and rail materials, showed the following under dry contact:

- Surface damage started within roughly 20,000 cycles, after which it remained substantially constant as the surfaces wore, suggesting an ideal test duration of ≈ 20,000 cycles.
- Presumed critical damage, in the form of surface pitting, occurred in the range T/N ≈ 0.15 through 0.3, above which an abrasive wear regime wore away the pitting as it formed.
- For Class C wheel material, a point of inflection occurred for wear between pitting and abrasive wear between T/N ≈ 0.2 and 0.3.

Contact stresses between unworn 36-inch AAR1B wheel and 136RE rail under 36-ton axle load and unlubricated conditions were modeled. So far, the results have been consistent with the results of the RCFS test program. Note that maximum contact pressure, pressure distribution, and resultant surface traction distribution can change with worn wheel and rail profiles and contact location; these cases will be investigated in the future. Using the given conditions, the following was concluded:

- A typical low rail tangential force environment for a lead axle of a nonsteering truck on an unlubricated track could cause permanent surface deformation on the surfaces of Class C wheels, Class D wheels, intermediate-strength rail at 0.1 T/N (occurred on 2-degree and sharper curves), and high-strength rail at 0.2 T/N (occurred on 3-degree and sharper curves).
- When tangential forces are zero, the maximum subsurface equivalent stress was approximately 106 ksi and was located approximately 3/16 inch below the surface. Subsurface von Mises stresses were slightly above Class C and below Class D wheel yield strengths. Intermediate-strength rail and high-strength rail yield strengths were higher than generated subsurface von Mises stresses.

5.1 Future Work

In addition to testing, a more accurate shakedown map will be regenerated based on modeling results supported with the RCFS test program. Plastic deformation prediction will be improved with nonlinear contact models. The modeling work will be funded under AAR SRI program.

With guidance from FRA, TTCI proposes to determine the surface roughness more accurately (depth of pitting), rate of wear, and point of inflection of wear for Class C and Class D wheels. The scope of work will include the following tests under low rail contact (the determined initiator of HIW):

- Class C and D wheels

- Balance and 3-inch underbalance conditions
- Finer T/N intervals with improved (more accurate) surface condition and wear measurements up to ≈ 20,000 cycles for T/N = 0.125, 0.150, 0.175, 0.20, 0.225, 0.250, and 0.275. These refined test intervals were within the control capabilities of the RCFS.
- Finer measurement and quantification of the surface damage
- Simulation of the seasonal effects of driving snow using an artificial third body layer

The T/N limits for surface damage between the two wear regimes of burnishing (presumed T/N < 0.15) and abrasive wear (presumed T/N > 0.3) will be determined from those tests. Results from those tests will support the determination of optimal T/N limits for the IFCT to avoid or substantially reduce the incidence of HIW and reduce low rail RCF damage in curves.

6. References

1. Cakdi. S. and Tournay, H. (2016, June). Integrated Freight Car Truck Curving: Part 1--Test Procedure. *Technology Digest* [TD-16-017]. Pueblo, CO: AAR/TTCI.
2. Johnson, K. (1985). *Contact Mechanics.* Cambridge, U.K.: Cambridge University Press.
3. Tournay, H., et al. (2015, June). The Root Causes for Wheelset Removals in Heavy Haul Service in North America. *Proceedings Of the 10th International Heavy Haul Conference.* Perth, Australia.
4. Vollebregt, E.A.H. (2016). User Guide for CONTACT, Rolling and Sliding Contact with Friction [Technical Report TR0-03, version 16.1]. Delft, The Netherlands: VORtech BV.
5. Tournay, H., and Anankitpaiboon, S. (2009, December). Wheel/Rail Forces Associated with the Formation of High Impact Wheels. *Technology Digest* [TD-09-040]. Pueblo, CO: AAR/TTCI.
6. Tournay, H.M. (2009, December). Review of the Mechanism for the Formation of Shells. *Technology Digest* [TD-09-041]. Pueblo, CO: AAR/TTCI.
7. Tournay, H., Guins, T., and Jones, M.C. (2011, October). Wheel life Comparison 3-piece versus M-976 Trucks. Case A: Two Train Sets of 135 cars in Western Coal Service. *Technology Digest* [TD-11-042]. Pueblo, CO: AAR/TTCI.
8. Tournay, H., et.al. (2011, Rev. December). Wheel Life Comparison 3-piece versus M-976 Trucks. Case B: 809 vs. 124 Cars in Western Coal Service. *Technology Digest* [TD-11-043]. Pueblo, CO: AAR/TTCI.
9. Tournay, H., Cakdi, S., and Jones, K. (2015, June). Damage Observed on the Treads of Wheels Removed from Revenue Service. *Technology Digest* [TD-15-014]. Pueblo, CO: AAR/TTCI.
10. Stock, R., et al. (2016). Material concepts for top of rail friction management—Classification, characterization and application. *Wear, 366,* 225–232.
11. Lewis, R., and Olofsson, U. (Eds.) (2009). *Wheel and Rail Interface Handbook – Chapter 9*. Amsterdam, The Netherlands: Elsevier.

Abbreviations and Acronyms

Abbreviation or Acronym	Name
AOA	Angle-of-Attack
AAR	Association of American Railroads
FRA	Federal Railroad Administration
FEA	Finite Element Analysis
HIW	High-Impact Wheel
IFCT	Integrated Freight Car Truck
IWS	Instrumented Wheelsets
LALR	Lead Axle Low Rail
RCF	Rolling Contact Fatigue
RCFS	Rolling Contact Fatigue Simulator
SRI	Strategic Research Initiative
T/N	Traction Ratio
TTC	Transportation Technology Center (the site)
TTCI	Transportation Technology Center, Inc. (the company)